

# A high resolution time-of-flight mass spectrometer for the detection of ultracold molecules

Stephan D. Kraft<sup>1\*</sup>, Jochen Mikosch<sup>1</sup>, Peter Staantum<sup>1,2\*\*</sup>, Johannes Deiglmayr<sup>1</sup>, Jörg Lange<sup>1</sup>, Andrea Fioretti<sup>3</sup>, Roland Wester<sup>1</sup>, Matthias Weidemüller<sup>1\*\*\*</sup>

<sup>1</sup> Physikalisches Institut, Universität Freiburg, Hermann-Herder-Straße 3, 79104 Freiburg, Germany

<sup>2</sup> Institut für Quantenoptik, Universität Hannover, Welfengarten 1, 30167 Hannover, Germany

<sup>3</sup> Istituto per i Processi Chimico-Fisici, C.N.R., via Moruzzi 1, 56124 Pisa, Italy

November 6, 2018

**Abstract** We have realized a high-resolution time-of-flight mass spectrometer combined with a magneto-optical trap. The spectrometer enables excellent optical access to the trapped atomic cloud using specifically devised acceleration and deflection electrodes. The ions are extracted along a laser beam axis and deflected onto an off axis detector. The setup is applied to detect atoms and molecules photoassociated from ultracold atoms. The detection is based on resonance-enhanced multi-photon ionization. Mass resolution up to  $m/\Delta m_{\text{rms}} = 1000$  at the mass of  $^{133}\text{Cs}$  is achieved. The performance of this spectrometer is demonstrated in the detection of photoassociated ultracold  $^7\text{Li}^{133}\text{Cs}$  molecules near a large signal of  $^{133}\text{Cs}$  ions.

## 1 Introduction

Applying ultracold atoms as targets for collision experiments with electrons, atoms, ions or photons requires sensitive ion detectors [1]. As an important example, in the study of ultracold ground state molecules formed from ultracold atoms an efficient and state-selective molecule detection scheme is based on resonance-enhanced multi-photon ionization (REMPI) [2] in combination with time-of-flight mass spectrometry.

Unlike many other experiments involving mass spectrometers, experiments with ultracold gases require a very good optical access. For example, in our setup we use more than 15 laser beams with beam diameters of up to 1.5 cm coming from different directions for trapping and manipulating the atomic cloud. Mass spectrometers employed to date in experiments with ultracold gases use simple electric field geometries for the extraction and detection of the ions. They offer good optical access at the expense of poor mass resolution ( $m/\Delta m \simeq 10$ ), which nevertheless is sufficient to separate homonuclear

alkali dimers [3, 4, 5] and in some cases also heteronuclear dimers from their atomic constituents [6, 7, 8, 9]. For photoassociation experiments of heteronuclear molecules with an unbalanced mass ratio of the atomic constituents or for the separation of different isotopomers, e.g.  $^{39}\text{K}^{85}\text{Rb}$  and  $^{39}\text{K}^{87}\text{Rb}$ , a high mass resolution is required. In order to discriminate nearby masses with largely different signal amplitudes this mass resolution needs to be near  $10^3$ .

Here we present an advanced time-of-flight mass spectrometer with higher resolution and good optical access for the detection of ions formed by ionization of trapped, ultracold atoms or molecules. High mass resolution is achieved by time focusing of the ions following a Wiley-McLaren scheme [10]. The field plates for accelerating the ions and the detector allow for optimal optical access to the region of the magneto-optical trap (MOT) as described in more detail below. Our motivation for this design was the selective detection of ultracold  $^7\text{Li}^{133}\text{Cs}$  molecules on a large background of  $^{133}\text{Cs}$  atoms, which we recently achieved with this spectrometer [18].

This article is organized as follows. In Sec. 2 the design of the time-of-flight spectrometer is presented. The experimental characterization is described in Sec. 3. In Sec. 4 we demonstrate the detection of ultracold LiCs molecules. A discussion is given in Sec. 5.

## 2 Design of the mass spectrometer

A time-of-flight (TOF) mass spectrometer [11] offers several advantages in experiments with cold atoms and molecules. With this type of spectrometer it is possible to record the whole mass spectrum at once, which is not the case for quadrupole or magnetic mass filters [12]. This allows one to monitor the development of the ratio of atoms to molecules, which can be helpful in optimizing production mechanisms for molecules. In addition, it is insensitive to magnetic fields, which are needed to operate magneto-optical or magnetic traps. As demonstrated by Wiley and McLaren [10] and employed in numerous experiments, e.g., with gas cells or molecular beams, the resolution of a time-of-flight mass spectrometer can be significantly improved by using a two step acceleration

\* s.kraft@fzd.de, now at Forschungszentrum Dresden-Rossendorf, Germany

\*\* now at Dept. of Physics and Astronomy, University of Aarhus, Denmark

\*\*\* m.weidemueller@physik.uni-freiburg.de

of the ions in electric fields of different strength created between three parallel field plates. By adjusting the ratio between the two field strengths it is possible to employ a time-focus, i.e. to minimize the arrival time spread of an ion cloud of given mass on an ion detector.

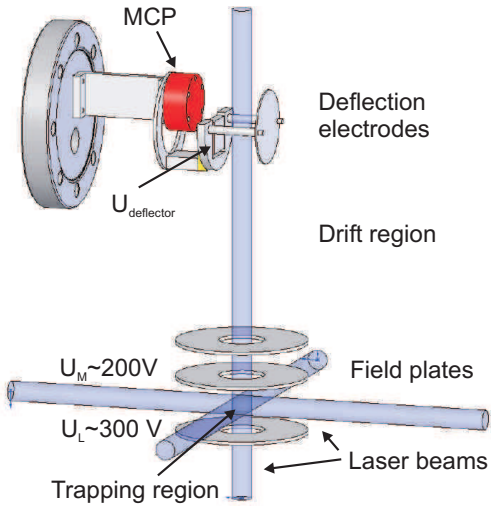


**Fig. 1** Drawing of the mass spectrometer (for dimensions see text). The ions are produced from a magneto-optical trap between the lower two plates and accelerated upwards. After drifting through a field free region of 30 cm they are deflected onto a microchannel plate detector. The setup allows optical access in the whole horizontal plane and along the vertical axis. The laser beams for the magneto-optical trap are indicated by three cylinders. More than 10 additional laser beams (not shown) also intersect the trapping region.

As shown in Fig. 1 the spectrometer for cold gases consists of two parts: an acceleration and a detection region. The acceleration is done by three horizontal field plates built around the magneto-optical trap from which the ions are produced. The stainless steel field plates are 2 mm thick, have a diameter of 80 mm, with a central hole of 30 mm diameter. No grids are mounted across the holes. The lower and the middle plate are separated by 40 mm and centered vertically around the MOT. The upper electrode is separated from the middle one by 20 mm. A voltage  $U_L = 300$  V is applied to the lower plate and voltages around  $U_M = 200$  V to the middle plate. The upper plate is grounded. This accelerates the ions upwards through the holes into the drift region.

After passing the field free drift region of 30 cm length, the ions arrive at the detection part of the spectrometer. This part is composed of a deflection electrode and a microchannel plate (MCP) detector attached on a single CF63 flange. The detector is mounted off the vertical axis to allow for optical access along this axis. The voltage applied to the deflector is typically -1.2 kV. A grounded grid is placed in front of the MCP to avoid background gas ions being pulled onto the detector.

As ion detector we use a matched pair of MCP plates (Burle Industries) [13]. The front of the first plate is held at a potential of -2.1 kV, the back of the second plate at -100 V. The produced electrons hit an anode plate behind the MCP connected to ground through a 100 k $\Omega$  resistor. AC signals from the anode are coupled out through a capacitance of 1 nF and referenced with 50  $\Omega$  to ground. A single ion arriving at the MCP produces a pulse of about 7 ns width at an amplitude of about 3 mV. The deflection electrode is mounted electrically isolated from the grounded plates using PEEK, which is a high quality plastic and sustains bake-out temperatures over 200°C without mechanical distortion and outgassing.

This design leaves full optical access in the entire horizontal plane, in planes tilted up to 30° from the horizontal and along the vertical axis. Compared to the theoretical resolution of  $m/\Delta m \simeq 4 \cdot 10^4$  given in [10] in our design the resolution is limited to about  $10^3$  by two effects as shown by simulations with SIMION [14]. The main decrease in resolution of about one order of magnitude is due to the deflection of the ions onto the detector in the upper part of the spectrometer. In addition, the configuration of the field plates around the trapping region leads to a factor of three decrease in mass resolution, because the large distance between the field plates and the large holes to accommodate the laser create a rather inhomogeneous acceleration field. To avoid this effect one could think of mounting grids across the holes. This would lead to interference effects of the laser beams passing through which would make an efficient cooling of the atoms impossible. Enlarging the outer diameter of the plates would reduce the optical access to the MOT which is needed for more than 15 laser beams including a 140 W CO<sub>2</sub> laser beam passing through the atomic cloud in the horizontal plane.

A more sophisticated electrostatic mirror such as a reflectron [15] would eliminate the influence of the deflector in the upper part of the spectrometer. In our experiment a free path of about 4 cm diameter in the vertical axis is necessary for 5 laser beams with 0.8 cm waist radius each. This makes the design of a grid-less reflectron [16, 17] very difficult and not worthwhile in an experiment with ultracold atoms since the already achieved resolution is more than sufficient.

### 3 Characterization

For the characterization of the mass spectrometer we produced Cs<sup>+</sup> ions from atoms in a MOT by photoionization with a pulsed dye laser (Radiant Dyes, Narrowscan, 7 ns pulse, 20 mJ/pulse, 20 Hz, operated at 716 nm). The MOT is loaded from a Zeeman-slowed atomic beam from a Cs oven. For these measurements, typically  $10^7$  Cs atoms are trapped at a particle density of  $10^{10}$  cm<sup>-3</sup>. In addition Cs<sub>2</sub> molecules are formed via photoassociation of the atoms using a cw Ti:Sapphire laser (Coherent

MBR 110) and ionized through REMPI using the pulsed dye laser [3]. Fig. 2 shows a typical measured time-of-flight spectrum for  $\text{Cs}^+$  and  $\text{Cs}_2^+$ . The atomic ions arrive  $21.2 \mu\text{s}$  after the ionization laser pulse, the flight time of the molecular ions is about 1.4 times longer, as expected from the square root of the mass ratio.

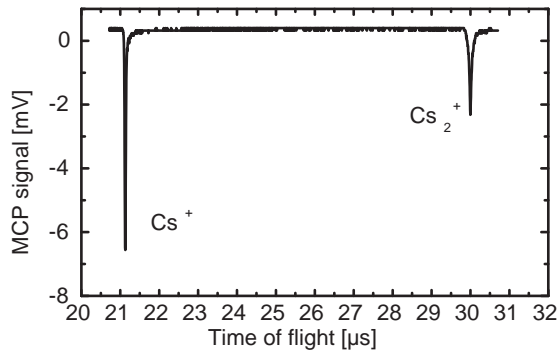


**Fig. 2** A measured TOF spectrum of  $\text{Cs}^+$  and  $\text{Cs}_2^+$ . The atomic ions arrive at the detector at  $21.2 \mu\text{s}$ , the molecular ions at  $29.7 \mu\text{s}$ .

To optimize the time focusing of the ions on the detector, we vary the ratio of the electric field strengths by applying a fixed voltage of  $U_L = +300 \text{ V}$  on the lowest field plate, keeping the upper one on ground and varying the voltage  $U_M$  applied to the middle plate. This measurement was done with only very few ions produced per pulse ( $< 15$ ), to avoid interaction among the ions through Coulomb repulsion and saturation effects of the MCP. Fig. 3 shows the rms peak width of the atomic ion signal for the atomic ions as a function of  $U_M$ . The width is extracted from an average of 128 single TOF traces. The signal depends strongly on the voltage  $U_M$  with a minimal rms peak width of about 10 ns at  $U_M = 202 \text{ V}$ . The peak width corresponds to a mass resolution of  $\frac{m}{\Delta m_{\text{rms}}} = 1000$ . This is in good agreement with the width of 15 ns obtained from the SIMION simulations. Fig. 3 shows that the voltages applied to the field plates have to be controlled on the one percent level for having optimal resolution.

Broadening of the signal due to Coulomb repulsion among the ions on their way to the detector is negligible for small ion numbers. However, it becomes the dominant broadening process for larger ion numbers. The influence of the Coulomb repulsion is investigated in two distinct ways. First, the number of ions produced in the extraction field is varied in a controlled way, second, a constant number of ions is produced in a field free environment and a variable delay between production and extraction of these ions is applied.

The number of ions, which is estimated from the peak area of the MCP signal, is varied by changing the power

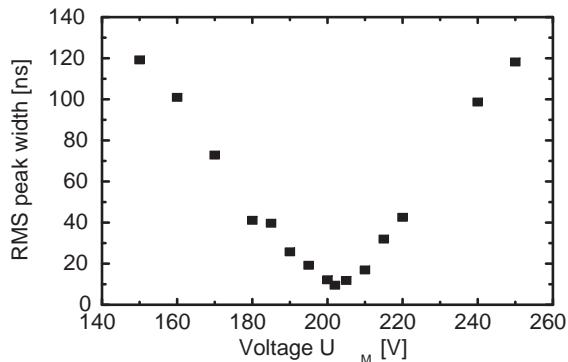


**Fig. 3** Time focusing of the ions on the detector by varying the voltage of the second field plate. A minimum width of 10 ns is achieved at a voltage of 202 V.

of the dye laser. The peak width increases with increasing ion number as shown in Fig. 4, hence the mass resolution decreases. The larger the ion number, the larger is the space charge density which leads to a stronger repulsion in the ionic cloud. Therefore the peak width on the detector grows with the number of produced ions. Since the ion number is varied by two orders of magnitude, special care must be taken to prevent saturation of the MCP for large ion numbers. Hence, we lowered the voltage applied to the MCP for larger ion intensities and used a relative calibration in order to compare the MCP signals at different MCP voltages.

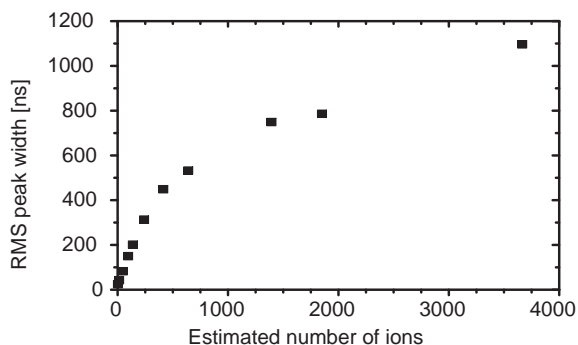


**Fig. 4** Peak width of the MCP signal for different ion numbers.

In a second measurement at a constant ion number, a variable delay is inserted between the time of production of the ions (time of dye laser pulse) and the beginning of their acceleration towards the detector. The voltages on the lower and middle field plates are switched with fast HV-switches (Behlke Electronic) and delays of 0-100  $\mu\text{s}$  are generated with a delay generator (Berkeley Nucleonics Corporation, Model 555 Pulse/Delay Generator).

This gives the ion cloud more time to expand under the influence of the Coulomb force and leads to a broader temporal distribution of the ions on the detector. Since the temperature of the ions is only a few hundred  $\mu\text{K}$  thermal energy can be neglected and the expansion is due to the Coulomb interaction only. For small ion numbers almost no effect is visible for small delay times (upper graph in Fig. 5). For delay times beyond  $40\ \mu\text{s}$  the signal becomes broader starting from less than  $25\ \text{ns}$  up to almost  $250\ \text{ns}$  after  $95\ \mu\text{s}$  delay. One would expect the peak area to be constant for a constant ion number. The observed increase is due to a reduced saturation of the MCP with increased delay time. This is here already the case for low ion numbers because of the small phase space volume occupied by the ions created from ultracold atoms. For large delays the ions hit a bigger area of the MCP and hence saturation is reduced. This saturation effect implies that the small rms peak widths measured at small delay times may even be overestimated. For large ion numbers (lower graph in Fig. 5) the peak width at zero delay is much larger than for the small ion numbers because the ions repel each other significantly on their way to the detector. The insertion of a delay has only little influence on the peak width, however, the total number of detected ions decreases rapidly. Under these conditions the strong Coulomb repulsion enlarges the cloud too much to map all ions onto the detector any longer and some of them hit the electrodes or the chamber walls.

#### 4 Detection of ultracold LiCs molecules

In this section the mass-spectrometric detection of ultracold LiCs molecules, recently observed for the first time [18], is described in detail. Due to the small LiCs signal levels, we switch for this purpose to a single ion counting configuration of the detector. Ultracold LiCs molecules are produced via photoassociation in a two species MOT containing Li and Cs atoms. Photoassociation is achieved by tuning a cw Ti:Sapphire laser ( $1/e^2$  radius of  $0.24\ \text{mm}$ , power =  $680\ \text{mW}$ ) to molecular resonances identified in previous spectroscopic studies [19], which leads to large signals in contrast to Ref. [18] where MOT light induced the photoassociation. The molecules are then ionized by two photons at  $696\ \text{nm}$  from a dye laser.

In order to reduce the number of  $\text{Cs}^+$  background ions arriving at the detector, we block the Cs-MOT lasers  $2\ \text{ms}$  before ionization using mechanical shutters. This guarantees that all Cs atoms are in the  $6S_{1/2}$  ground state and therefore three photons are necessary for their ionization. Fig. 6a shows 350 single TOF traces of a pure  $\text{Cs}^+$  sample plotted on top of each other together with the average signal. In this plot two different features are visible: a sharp peak at  $21.90\ \mu\text{s}$  and a broad distribution of ions arriving roughly from  $21.3\ \mu\text{s}$  to  $22.8\ \mu\text{s}$ . While the

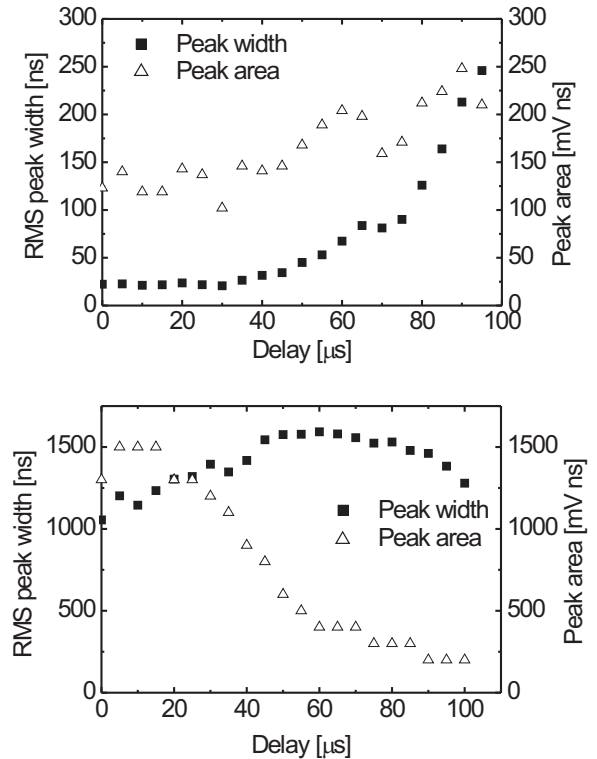


**Fig. 5** Coulomb repulsion for about 10 ions (upper) and more than 150 ions (lower).

sharp peak (width  $\sim 80\ \text{ns}$ ) is caused by initially cold Cs atoms from the MOT, we attribute the broad distribution (width  $\sim 500\ \text{ns}$ ) to fast Cs ions produced by ionization of photo-dissociated  $\text{Cs}_2$  molecules<sup>1</sup> [18]. A  $\text{Cs}_2$  molecule can be dissociated by a photon of the ionization laser transforming it into a pair of Cs atoms either in the  $6S_{1/2}+6P_{3/2}$  or the  $6S_{1/2}+6P_{1/2}$  states. Each cesium atom moves with  $0.18\ \text{eV}$  or  $0.22\ \text{eV}$  kinetic energy, depending on the asymptote. Ionization of the fast Cs( $6p$ ) atoms by two additional photons leads to ions arriving up to about  $300\ \text{ns}$  earlier or later compared to the time-of-flight peak of the cold cesium atoms. The distribution of the arrival times reflects the angular distribution of the fragment velocities of the Cs( $6p$ ) atoms that emerge from the  $\text{Cs}_2$  photodissociation. The measurement of such arrival time distributions is expected to open up new opportunities for the study of quantum-state specific properties of ultracold molecules.

These fast ions constitute a significant background at the expected arrival time of  $22.47\ \mu\text{s}$  for the LiCs ions. We therefore modified the voltage settings in the following way: larger absolute values of voltages lead to an improved energy focusing; changing the ratio of the field plate voltages  $U_L/U_M$  allows us to shift the arrival of

<sup>1</sup> These  $\text{Cs}_2$  molecules are formed from cold Cs atoms by photoassociation through the cooling lasers.

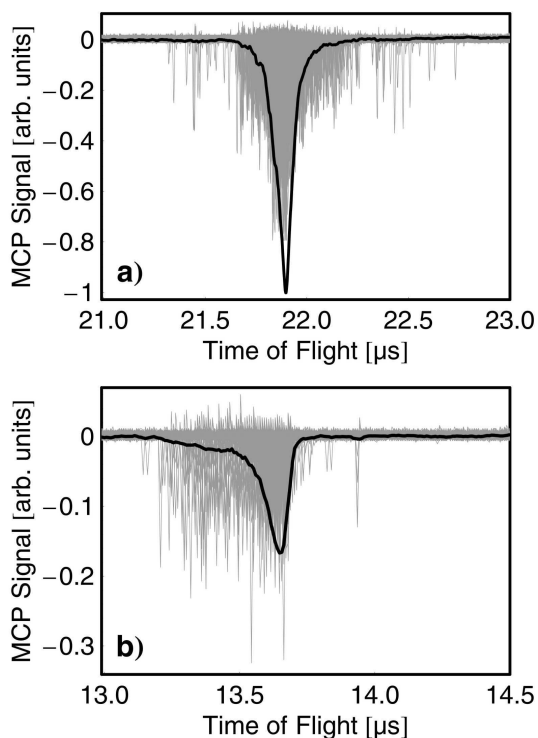


**Fig. 6** Time of flight trace around the arrival time of  $\text{Cs}^+$  ions. Shown are an overlay of 350 individual traces (grey) and the averaged signal (black) (enlarged by a factor of 10 for visibility). Two different set of voltages are applied for a) optimal time focusing and b) increase selectivity for masses above  $^{133}\text{Cs}$

the fast ions to earlier times at the cost of none-optimal time focusing. Fig. 6b shows a modification ( $U_L=800\text{ V}$ ,  $U_M=610\text{ V}$ ) where the arrival time of nearly the entire signal produced by fast  $\text{Cs}^+$  ion has been shifted to a time before the cold  $\text{Cs}^+$  ions arrive. Therefore it is now possible to detect even small numbers of ions with a slightly higher mass than  $\text{Cs}^+$  with almost no background contribution from the fast  $\text{Cs}^+$  ions.

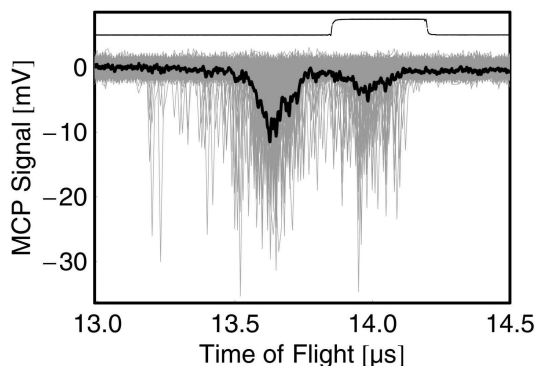


**Fig. 7** Overlay of 600 individual time of flight traces (grey), averaged signal (black) and window set for detection of  $\text{LiCs}^+$  (dashed line).

Fig. 7 shows the two well separated signals from roughly 1,000  $\text{Cs}^+$  and about 300  $\text{LiCs}^+$  ions. For the counting of  $\text{LiCs}$  molecules, only the ions appearing in a gated time window of 350 ns around the expected arrival time of  $\text{LiCs}^+$  are detected by a fast discriminator and a counter. The gate was chosen carefully to avoid a background caused by fast  $\text{Cs}^+$  ions. The modified set of voltages reduces the number of fast  $\text{Cs}^+$  ions arriving in the time window set for detection to less than one per 100 shot which allows us to measure even small numbers of formed  $\text{LiCs}$  molecules.

## 5 Discussion

The mass spectrometer for ultracold atomic and molecular gases presented here yields optimal optical access to the trap region with a mass resolution of  $\frac{m}{\Delta m} = 1000$  in good agreement with design simulations. For large ion numbers, however, the mass resolution is decreased due to Coulomb repulsion between the ions during their flight time. Therefore, one has to adjust the ion intensity to optimize signal strength versus mass resolution and suppress unwanted ions (e.g., atomic cesium). In this work this has been achieved by blocking the Cs excitation lasers prior to ionization. A further reduction can either be done by pushing away the atoms with a resonant laser before ionizing the molecules or by switching on the deflection electrode after the atomic ions have passed through the deflector region.

We demonstrate the capability of this setup to distinguish between atomic  $\text{Cs}^+$  and molecular  $\text{LiCs}^+$  ions produced from a two-species MOT [20] setup via photoassociation. This spectrometer will be useful for experiments studying ultracold chemical reactions, such as the quantum-state resolved detection of products of the  $\text{Li} + \text{Cs}_2$  exchange reaction.

This work is supported by the Deutsche Forschungsgemeinschaft in the Schwerpunktsprogramm 1116 "Interactions in Ultracold Atomic and Molecular Gases" under WE-2661/1-2 and 1-3. P. S. and J. D. are supported by the EU Research Training Network "Cold Molecules" under the Contract No HPRN-2002-00290. The stay of A. F. in Freiburg was supported by the CATS network of the European Science Foundation and the Cold Molecules Network. J. D. acknowledges financial support from the German-French University, Saarbrücken.

## References

1. J. Ullrich and V. P. Shevelko, editors, *Many-Particle Quantum Dynamics in Atomic and Molecular Fragmentation*, Springer, 2003.
2. G. Petty, C. Tai, and F. W. Dalby, *Phys. Rev. Lett.* **34**, 1207 (1975).

3. A. Fioretti, D. Comparat, A. Crubellier, O. Dulieu, F. Masnou-Seeuws, and P. Pillet, *Phys. Rev. Lett.* **80**, 4402 (1998).
4. C. Gabbanini, A. Fioretti, A. Lucchesini, S. Gozzini, and M. Mazzoni, *Phys. Rev. Lett.* **84**, 2814 (2000).
5. A. N. Nikolov, E. E. Eyler, X. T. Wang, J. Li, H. Wang, W. C. Stwalley, and P. L. Gould, *Phys. Rev. Lett.* **82**, 703 (1999).
6. A. Kerman, J. M. Sage, S. Sainis, T. Bergeman, and D. DeMille, *Phys. Rev. Lett.* **92**, 153001 (2004).
7. M. W. Mancini, G. D. Telles, A. R. L. Caires, V. S. Bagnato, and L. G. Marcassa, *Phys. Rev. Lett.* **92**, 133203 (2004).
8. D. Wang, J. Qi, M. F. Stone, O. Nikolayeva, H. Wang, B. Hattaway, S. D. Gensemer, P. L. Gould, E. E. Eyler, and W. C. Stwalley, *Phys. Rev. Lett.* **93**, 243005 (2004).
9. C. Haimberger, J. Kleinert, M. Bhattacharya, and N. P. Bigelow, *Phys. Rev. A* **70**, 021402 (2004).
10. W. C. Wiley and I. H. McLaren, *Rev. Sci. Instr.* **26**, 1150 (1955).
11. C. Weickhardt, F. Moritz, and J. Grotemeyer, *Mass Spectrometry Reviews* **15**, 139 (1996).
12. W. Paul, H. P. Reinhard, and U. von Zahn, *Z. f. Physik* **152**, 143 (1958).
13. J. L. Wiza, *Nucl. Instr. and Meth.* **162**, 587 (1979).
14. SimIon 3D Version 7.0, Idaho National Engineering and Environmental Laboratory.
15. U. Boesl, H. J. Neusser, R. Weinkauff, and E. W. Schlag, *J. Phys. Chem* **86**, 4857 (1982).
16. R. Frey, G. Weiss, H. Kaminski, and E. W. Schlag, *Z. Naturforsch.* **40a**, 1349 (1985).
17. R. P. Schmid and C. Weickhardt, *Int. J. Mass Spectrom.* **206**, 181 (2001).
18. S. D. Kraft, P. Sta anum, J. Lange, L. Vogel, R. Wester, and M. Weidemüller, *J. Phys. B* **39**, S993 (2006).
19. P. Sta anum, A. Pashov, H. Knöckel, and E. Tie mann, *Phys. Rev. A* **75**, 042513 (2007).
20. U. Schlöder, H. Engler, U. Schünemann, R. Grimm, and M. Weidemüller, *Eur. Phys. J. D.* **73**, 802 (1999).